YU ISSN 0015—3206
FZKAAA 20 (4) 421 (1988)

ELECTRON-IMPACT EXCITATION OF KRYPTON AT INCIDENT ELECTRON ENERGY OF 60 eV

DUŠAN FILIPOVIĆ*, VLADIMIR PEJČEV, BRATISLAV MARINKOVIĆ and LEPOSAVA VUŠKOVIĆ

Institute of Physics, P. O. Box 57, 11001 Beograd, Yugoslavia

Received 29 December 1987

UDC 539.186

Original scientific paper

Normalized, absolute differential cross sections (DCS's) have been measured for the 5s $[3/2]_1$, 5s' $[1/2]_1$ and 5p $[1/2]_0$ states of krypton at incident electron energy of 60 eV. Energy resolution of the spectrometer was approximately 50 meV, and scattering angles ranged from 10° to 150°. These DCS's have been measured for the first time in wide angular range, because of their importance for studying alignment and orientation of atomic states in collisional processes. The properties of the electron-impact spectrometer used is outlined.

1. Introduction

Electron-impact excitation of the larger-atomic-number noble-gas atoms is a very instructive way of understanding excitation mechanisms in atomic collisional processes. The dimensionless alignment and orientation parameters are convenient for visualizing the shape and dynamics of the atomic outer shell charge cloud. This investigation of electron-impact excitation of krypton at 60 eV incident electron energy was suggested by Andersen[1]; although coherence and correlation analysis have been done[2,3], only theoretical differential cross sections (DCS's) were available[4].

* Permanent address: Technical Faculty, Novi Sad University, 21000 Novi Sad, Yugoslavia

For testing of theoretical predictions DCS measurements of clearly resolved electronic states are needed. From the experimental point of view the main problem associated with the inelastic DCS measurements is the rapidly decreasing signal intensity as the scattering angle increases from 0°, at the energy of interest (60 eV).

At 60 eV incident-electron energy Lewis et al.[5] measured the relative DCS for the unresolved 5s states. Delage and Carette[6] measured the energy-loss spectra for scattering angles ranging from 0° to 60°, and determined absolute values of the optical oscillator strenghts by normalizing their relative data to the absolute values obtained by Ganas and Green[7]. Same authors[8] measured relative DCS's for a number of states, but in the same limited angular range. Meneses et al.[4] applied first-order many-body theory to calculate DCS's for the first four s-states. In addition they calculated electron-photon coincidence parameters for the optically allowed states. Bartschat and Madison[9] derived distorted wave Born approximation for the DCS's calculation. They also calculated angular correlation parameters for the electron-impact excitations.

The spectrometer used in these measurements on krypton has been already used in the investigation on Ar[10], Xe[11], N_2O[12], H_2S[13], and O[14,15], but only a brief description of the apparatus was given until now[11,12].

In Section 2. we describe the apparatus. Rather than describing in detail the electron optics, we would like to compare calculated[16] (on the basis of fundamental electron-optical relations) values of charge limited currents and typical values which were obtained in our experimental conditions. In Section 3. the experimental procedure for inelastic DCS measurements is explained. Our results as well as comparison with other available data are presented in Section 4. Finally, in Section 5. discussion and conclusion are given.

2. *Apparatus*

The apparatus is designed to satisfy the following conditions: a) a high vacuum interaction region, without magnetic as well as electric fields, b) a collimated atomic beam for the »cross-beam« experimental technique, c) a narrow monoenergetic incident electron beam, d) both high energy resolution and high angular resolution analysis of scattered electrons in a wide angular range, e) an »energy-loss« mode of operation of the electron optics, and a simple transition to an »impact-energy« mode for the energy scale calibration and f) a single-electron detection, processing by a pulse technique, and data storage for a further computer elaboration.

Scheme of the vacuum and gas-inlet system is shown in Fig. 1. Differential pumping of the shielding boxes for protection of the electron optics (M and A) with respect to the vacuum chamber C, is provided by two oil diffusion pumps DP1 and DP2, respectively. A background pressure, measured at the top of the chamber, of the order of 5 μPa is achieved. Standard diffusion pump cooling and protection equipment, as well as mechanical pump MP, are built in. A probe gas (PG) and a sample gas (SG) can be injected into the chamber through a 0.05 mm individual diameter and 5 mm long capillary array N, which is fixed to the arm of the analyzer and rotates with it. This ensures a constant position of the atomic beam in respect to the analyzer.

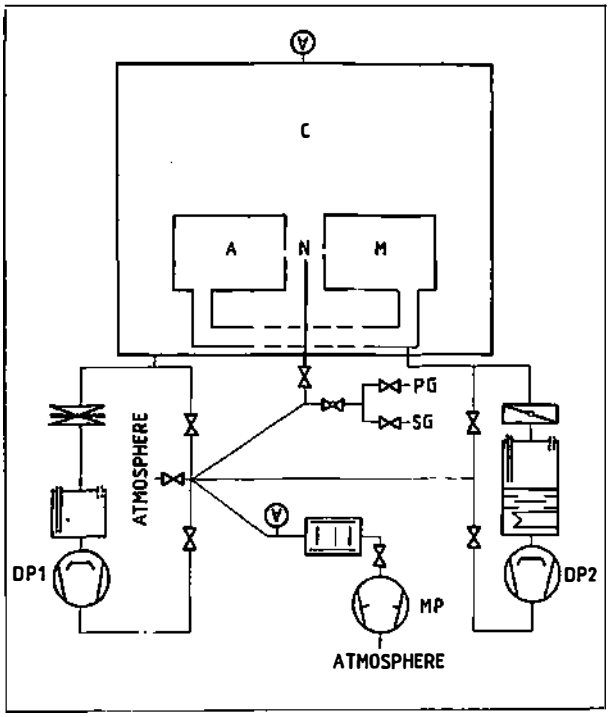

Fig. 1. Scheme of the vacuum and gas system (explanation in the text).

To minimize the external magnetic field influence, double μ-metal shield is built into the chamber. The residual magnetic field in the centre of the chamber is less than 0.1 μT. All of the electrodes were made of oxygen-free high-conductivity (OFHC) gold-plated copper. The hemispheres and apertures were made of molybdenum. All materials used inside the chamber were carefully checked to be non-magnetic. All insulators used along the electron beam path are shielded, and all surfaces were kept clean in order to minimise a collection of electrons and an electrostatic field appearance. Additional improvement of the cleansiness by baking the electron optics to about 450 K is achieved.

Scheme of the electron optics is shown in Fig. 2. The system consists of two parts, that is the monochromator and the analyzer, which are arranged as simple changable modules. Both the monochromator and the analyzer are systems of cylindrical electrostatic lenses with hemispherical dispersion elements. Using an arrangement with horizontal trajectories of electrons in the monochromator, and at an angle of 45° with respect to the horizontal plane in the analyzer, scattering angles from $-30°$ to $+150°$ can be achieved. The design of the electron optics is based on principles systematically given in unpublished lectures by Kuyatt[17]. Geometries and focal properties of the electron lens systems have been calculated by Chutjian[16]. Rather than giving a detailed description, we would like to compare values of charge limited currents calculated by Chutjian[16], and typical values of currents which were obtained in our experimental conditions.

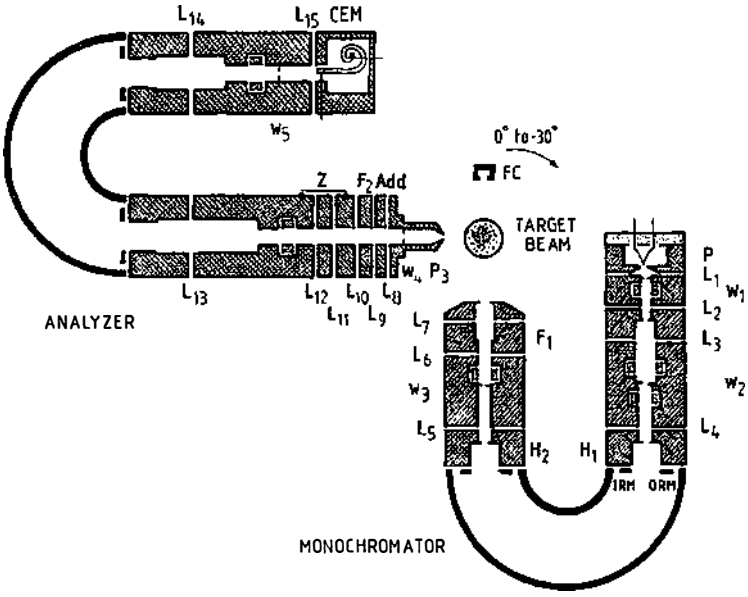

Fig. 2. Scheme of the electron optics (explanation in the text).

The monochromator produces a monoenergetic electron beam in the horizontal direction and focuses it onto a target atomic beam perpendicular to the horizontal plane. The electron source, P, is of the Pierce type with a tungsten hair pin cathode. The Pierce source illuminates the window w_1. This structure can be treated as a Calbick lens of a focal length $f = -4d$, where d is the distance from the window to the top of the cathode. The beam angle at w_1 (of radius r_1), from the geometrical considerations, is

$$\Theta_b \cong \operatorname{tg} \Theta_b = r_1/4d. \tag{1}$$

The pencil angle at w_1 is a quotient of the normal and parallel components of electron velocity with respect to the optical axis. For the normal electron energy distribution near the cathode ($E_c = 0.1$ eV)

$$\Theta_p \cong \operatorname{tg} \Theta_p = \sqrt{E_c/eV_1}, \tag{2}$$

where V_1 is the potential at w_1. For $r_1 = 0.4$ mm, $d = 3.6$ mm and the typical value of $V_1 = 100$ V (for the incident electron energy of 20 eV), formulae (1) and (2) give $\Theta_b = 0.028$ rad ($\cong 1.6°$) and $\Theta_p = 0.032$ rad ($\cong 1.8°$), approximately.

The space charge limited current from the cathode, at w_1, given by the Child's formula, is

$$I_1 = 7.32\,[V_1\,(\mathrm{V})]^{3/2}\,(r_1/d)^2\,(\mu\mathrm{A}). \tag{3}$$

One obtains $I_1 = 8 \times 10^{-5}$ A. The measured currents in the monochromator typically is 5×10^{-5} A, which is in satisfactory agreement with the calculated value.

In the monochromator the image of w_1 is focused at w_2 by means of collimator lens system L2-L3. Electrons must then be deccelerated to an energy low enough to disperse well by the hemispheric field. This is the role of L4 lens which focuses an image of w_2 at a virtual aperture placed at the entrance plane of the hemispheres. Since the current is conserved along the path from the cathode to the entrance plane of the hemispheres, Liouville's theorem about the remaining constant density of points in phase space can be used. It can be subtitled as the two dimensional Helmholtz-Lagrange law for two planes (at w_1 and w_2),

$$r_1 \Theta_{p_1} \sqrt{V_1} = r_2 \Theta_{p_2} \sqrt{V_2}, \tag{4}$$

where: r_2 — radius of the w_2,

Θ_{p_2} — pencil angle at the w_2, and

V_2 — potential at w_2.

For the r_1, Θp_1 and V_1 values already given, and the $r_2 = 0.4$ mm and a typical value $V_2 = 40$ eV, pencil angle Θ_{p2} value of 0.05 rad ($\cong 3°$) has been obtained.

A pupil between the w_2 and the hemispheres, designed by Chutjian[16], is omitted in our arrangement because we need higher current rather than very low aberation due to low pencil angle at the virtual aperture.

From simple geometrical cosiderations, radius of virtual aperture at entrance plane of the hemispheres can be obtained as

$$x_1 = r_2 + f \operatorname{tg} \Theta_{p_2} \cong r_2 + f \Theta_{p_2} \tag{5}$$

when the w_2 is at focal length ($f = 13$ mm) of L4-lens. For the values mentioned above, relation (5) gives $x_1 = 0.5$ mm approximately. This result is important for examining the hemispherical deflector energy resolution.

The hemisperical deflector focuses the virtual aperture at entrance plane onto its exit plane with magnification of 1. Electrostatic field $\varepsilon(r)$, between the concentric hemispheres of radii R_2 and R_1 ($R_1 \ll R_2$) is a function of $1/r^2$. Traveling of electrons of energy $E_0 = eV_0$ in a circle of radius $R_0 = (R_1 + R_2)/2$, can be achieved with potential difference between the hemispheres

$$-\Delta V = V_0 (R_2/R_1 - R_1/R_2). \tag{6}$$

Obviously, the quotient $-\Delta V/V_0$ is a constant for a hemispherical deflector and takes the value of 1.40 for the deflector used. Relation

$$-(V_0 - V_1) = \int_{R_1}^{R_0} \varepsilon(r)\, \mathrm{d}r \tag{7}$$

gives potential of the inner sphere

$$V_1 = V_0 (2 - R_1/R_2). \tag{8}$$

Similarly, for the potential of the outer sphere

$$V_2 = V_0 (2 - R_2/R_1). \tag{9}$$

Analysis of dynamics of an electron starting at x_1 radial distance near R_0 and angle α with respect to path of radius R_0, shows that the electron leaves at x_2 radial distance at the exit plane, given by

$$x_2/R_0 = -x_1/R_0 + 2\Delta E_{1/2}/E_0 - 2\alpha^2. \tag{10}$$

For low α, and $x_1 = x_2 = w/2$

$$\Delta E_{1/2}/E_0 = w/2R_0. \tag{11}$$

This relation is usualy used for description of hemispherical deflector as dispersion element in electron optics. For $w = 1$ mm, and $E_0 = 2$ eV, thus the energy resolution of 0.02 eV can be estimated. Energy resolution of the spectrometer, as full width at half maximum of lines in a number of energy-loss spectra of 40 meV, is in good agreement with estimated value of sum of the monochromator and the analyzer resolutions. Two rings ORM and IRM, as well as Herzog-correction electrodes H1 and H2, minimize boundary effects of the hemispheres. After leaving the space between hemispheres, accelerating as well as focusing of the beam at aperture w_3 by L5 lens takes place. Lens L6-L7 (as a zoom-lens) focuses electron beam to the interaction centre independently of the electron energy.

The analyzer optics consists of two entrance apertures p_3 and w_4, which define acceptance angle for scattered electrons. Lens L8 is an »energy-add« lens. In the energy-loss mode of operation of the spectrometer this lens adds back an amount of energy to the accepted electrons which they have lost in the collision. In this way electrons have the same energy in the analyzer over an energy-loss scan. The main result is a constant electron transmission of the analyzer. That is, line-intensity ratios in energy-loss spectra are kept constant. Lens L9-L10 (as a zoom-lens) compensates for small changes of the add-lens properties with the electron energy. Lens L11-L12 is an einzel-lens (aplied here as a field lens) and ensures zero beam angle for electrons deccelerated by L13-lens, at entrance plane of the hemispheres. The hemispherical deflector of the analyzer, as well as both inner and outer ring, are the same as in the monochromator. Electrons are accelerated and focused at aperture w_5 by L14-lens. Finally, electrons are focused into the electron multiplier (in the single electron detecting mode) by L15-lens.

Electrical pulses obtained in RC-circuit of the multiplier are processed by a standard pulse technique: preamplifier, amplifier, counter, ratemeter and multichannel analyzer. The data are both recorded on a X-Y plotter and stored on punched tapes for further computer processing.

To establish the energy scale without a shift due to contact potentials, the spectrometer was built to enable easy transition from the energy-loss mode to the impact-energy mode of operation. Electrical scheme of the spectrometer is shown in Fig. 3. In the energy-loss mode potentials of all the analyzer electrodes and the detector, with respect to the ground, are swept linearly for energy loss. This is necessary in order to keep the angular characteristics of the beam as well as posi-

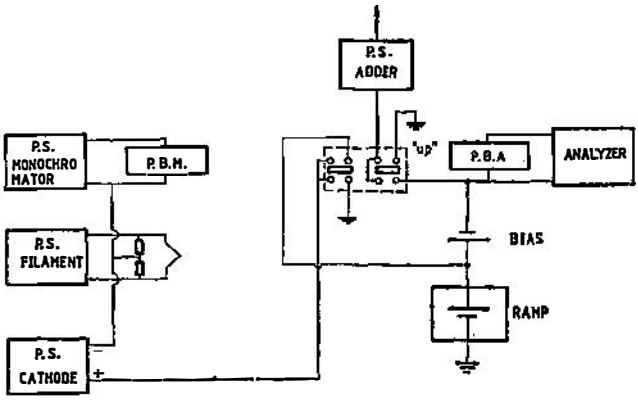

Fig. 3. Scheme of the electrical system. The »Up« switch position ensures the impact-energy mode, and the opposite position ensures the energy-loss mode of operation of the spectrometer.

tions and sizes of images, unchanged. Potentials of electrodes F2 and Z are swept linearly, which is acceptable when the three-element zoom-lens L9-L10 works in high potential mode. In case of the Z-potential, the linear (instead non-linear) sweep restricts the region of energy-loss to a few eV for obtaining true intensity ratios from the energy-loss spectra. In the impact-energy mode of operation of the spectrometer, the energy must be swept linearly, but the F1 as well as the F2 and the Z potentials must be swept non-linearly. Add-potential must be constant with respect to the ground potential. These special conditions have not yet been established in our experiment, however this mode of operation enables the energy scale calibration on the basis of the position of the resonance at 19.38 eV in the elastic electron scattering on helium.

Mechanical system of the spectrometer enables rotation of the analyser by a hand-movable cog-wheel transmission.

3. *Experimental procedure*

The DCS measurements were performed in a crossed beams technique. An atomic beam collimated by the capillary array, was crossed perpendicularly by a monoenergetic electron beam. The scattered electrons were analyzed by the rotatable (from —30° to 150°) analyzer system. For a given position of the analyzer the addition of energy to the inelastically scattered electrons is achieved by sweeping the analyzer potential. If that addition is equal to the energy-loss of incident electrons due to the excitation of target atoms to a particular electronic state, a line in the energy-loss spectrum appears. Density of the atomic beam was kept low enough so that the signal intensity versus the pressure was linear in this domain of density. It means that double scattering of electrons on atoms can be neglected.

Both the energy-loss spectra analysis and the direct angular distribution measurements were used in this work.

The zero scattering angle was determined from the symmetry of the angular distribution in the range of $-30°$ to $30°$ before each measurement.

The energy scale was calibrated in these measurements by means of the position of the well known helium resonance at 19.38 eV, and uncertainty in the energy is estimated to be within 0.2 eV.

The angular resolution has been taken to be the angle at which the intensity of the incident electron beam, measured by the analyzer, fails to half maximum. In practice, during the angular resolution measurements, the emission from the cathode was remarkably reduced and the gas did not enter into the chamber. As a detector we used the analyzer rotated trough an angle from the straight-through position to angles at which the electron count rate to the multiplier falls to zero, both sides. The angular resolution obtained was better than $\pm 1°$.

The optimization of the electron optics was done in such a way that it provides an energy resolution high enough to resolve the lines in the energy-loss spectra, but at the same time assuring a count rate which yields the statistical errors within 10%. The optimal conditions correspond also to a minimal change of the intensity ratios of lines when the focusing conditions change. This is important especially when dealing with elastic-reference inelastic ($5s\ [3/2]_1$) intensity ratio measurements needed for inelastic DCS's absolute scale determination.

To establish the inelastic DCS's absolute scale we measured the angular intensity distribution of electrons elastically scattered on krypton atoms at 60 eV impact energy[18]. The absolute elastic of DCS at 30° scattering angle was obtained by interpolation DCS values at 50 eV and 75 eV impact energy obtained by Srivastava et al.[19]. Rather than transmission of the analyzer we measured »relative transmission«, that is the ratio of the intensities of a given peak, under two conditions: when some other peak is focussed and when the observed one is focused alone. The same relative transmissions were obtained for the reference inelastic peak with respect to elastic peak as well as for the elastic peak with respect to the reference inelastic peak. In this way, the elastic-to-reference inelastic intensity ratio was determined as $I_{el}/I_{inel} = 46$ at 30° scattering angle. Finally, on the basis of the elastic-to-reference inelastic as well as given inelastic-to-reference inelastic intensity ratios, the inelastic DCS absolute scale for a separate state was determined.

4. *Results*

We have measured angular intensity distribution of electrons elastically scattered on krypton atoms at 60 eV impact energy[18]. Scattering angle was changed from 10° to 150°. Relative DCS, as the arithmetic mean value of at least three angular distributions, mutually normalized with respect to a relative value of a local maximum, was determined. The relative DCS value at 30° scattering angle was normalized with respect to the results by Srivastava et al.[19].

The absolute DCS values for the $5s\ [3/2]_1$ state were obtained by using our normalized elastic DCS and the elastic-to-reference inelastic intensity ratio obtained in a separate experiment as explained in Section 3. These values are presented in Fig. 4, in the angular range from 10° to 150° by smooth curve drown through the circles.

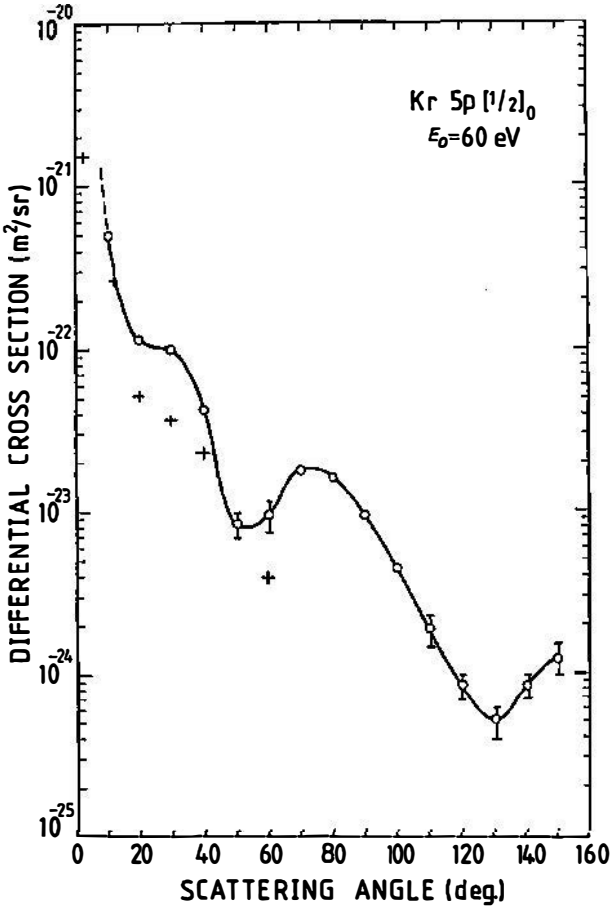

Fig. 4. Differential cross sections for the 5s $[3/2]_1$ state: +, Delage and Carette (Ref. 8); ..., Meneses et al. (Ref. 4); —, Bartschat and Madison (Ref. 9); —O—, present result.

The absolute DCS values for the 5s' $[1/2]_1$ state were obtained on the basis of DCS value of 5s $[3/2]_1$ reference state at 30° scattering angle as well as separatelly measured the inelastic-to-reference inelastic intensity ratio at the same angle, for which we found the value of 0.72. These inelastic DCS values are presented in Fig. 5, with smooth curve drown through the circles.

The absolute DCS values for the 5p $[1/2]_0$ state were obtained in a similar way, as the DCS values for the 5s' $[1/2]_1$ state. In a separate experiment we found the inelastic-to-reference inelastic intensity ratio to be 0.068 at 9° scattering angle. The inelastic DCS value was calculated then as a product of this ratio and DCS for 5s $[3/2]_1$ state extrapolated to the same angle. (We found the value of $16 \times \times 10^{-21}$ m^2/sr for 5s $[3/2]_1$ state, at 9°). Normalized DCS values for the 5p $[1/2]_0$ state are shown in Fig. 6 with the smooth curve drown through the circles.

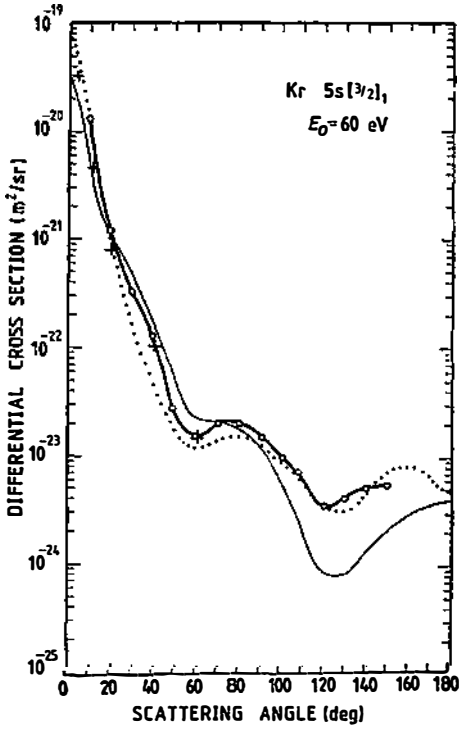

Fig. 5. Same as Fig. 4. but for the 5s' $[1/2]_1$ state.

In Table 1 normalized absolute DCS values for the 5s $[3/2]_1$, 5s' $[1/2]_1$ and 5p $[1/2]_0$ states are presented numerically.

Estimations of the maximum error for each of the investigated features were performed under the following conditions. A contribution to the systematic error due to uncertainty of the energy is within 3%. The uncertainty of the angular scale of $\pm 1°$ contributes to the error for the relative inelastic DCS less than 5%. Statistical errors were always within 10% in individual measurements. In a few cases, in which there were larger statistical errors due to very low signal intensity, the results are shown in figures with statistical error bars of the data points.

The total error for the elastic DCS as well as the normalization procedure for the reference inelastic DCS, contributes less than 35% to the error for the absolute DCS of the reference inelastic feature.

On the basis of the estimated errors mentioned above, the »level of error« as the square root of the sum of squares, for the reference inelastic DCS (5s $[3/2]_1$ state), was found to be 37%.

An inelastic-to-reference inelastic intensity ratio determination contributes an additional error of less than 10% to the error of the absolute DCS. Thus the »level of error« for the 5s' $[1/2]_1$ state of 38% can be estimated.

For the 5p $[1/2]_1$ state statistical error contributes less then 20% to the total error and the »level of error« of 42% can be estimated.

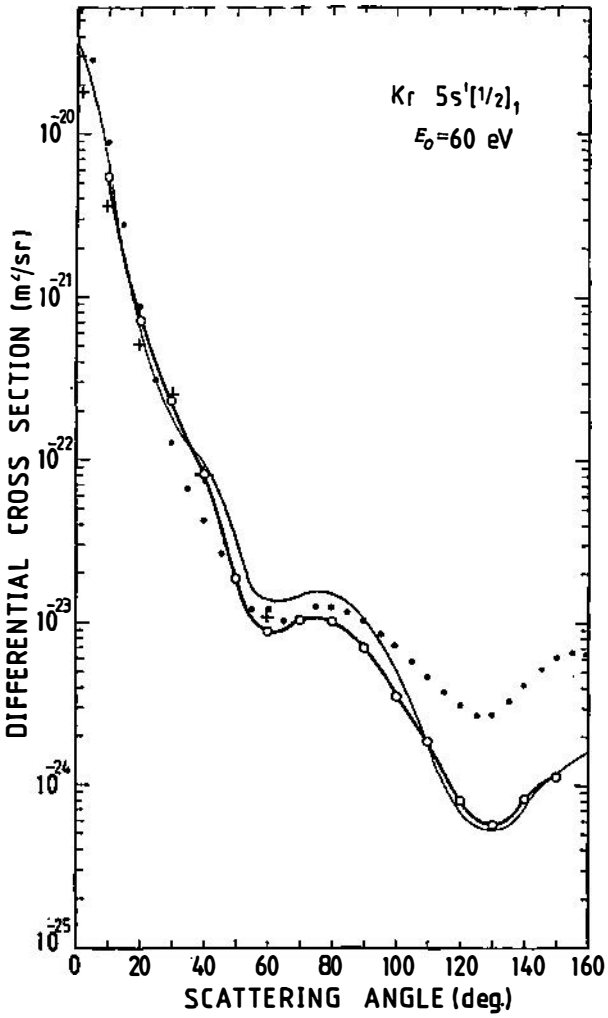

Fig. 6. Same as Fig. 4. but for the 5p $[1/2]_0$ state.

5. *Discussion and conclusion*

The krypton ground state has an electron configuration:

$$1s^2 2s^2 2^6 p 3s^2 3p^6 3d^{10} 4s^2 4p^6.$$

The excited electronic states investigated in this work: 5s $[3/2]_1$, 5s' $[1/2]_1$ and 5p $[1/2]_0$, are formed by an electron impact by transition of the 4p-electron. The states denoted by 51 correspond to the value of $J_c = 3/2$ angular momentum of the Kr^+ ion core, and the state 51' corresponds to the value of $J_c = 1/2$.

TABLE 1.

State	$5s\ [3/2]_1$	$5s'\ [1/2]_1$	$5p\ [1/2]_0$
Θ (deg.)			
10	1300	550	50.0
20	109	72.5	11.8
30	33.5	23.5	10.1
40	11.9	8.1	4.35
50	2.53	1.85	0.85
60	1.32	0.89	0.96
70	1.95	1.05	1.80
80	1.88	1.02	1.68
90	1.39	0.72	0.96
100	0.832	0.36	0.45
110	0.778	0.19	0.19
120	0.381	0.082	0.087
130	0.460	0.059	0.052
140	0.541	0.083	0.083
150	0.566	0.14	0.12

Differential cross sections for inelastic scattering of electrons on Kr, at 60 eV impact energy in units of 10^{-23} m^2/sr.

Generally speaking, the DCS curves for s-states are forward-peaked. It means that a long range coulombic interaction is predominant with respect to a short--range exchange interaction.

For the $5s\ [3/2]_1$ state, the first-order many-body theory (FOMBT) calculation by Meneses et al.[4] provides a better agreement in shape with our experimental results than the distorted wave Born approximation (DWBA) of Bartschat and Madison[9].

For the $5s'\ [1/2]_1$ state agreement between our DCS results and FOMBT results by Meneses et al.[4] is better than between our DCS results and DWBA results by Bartschat and Madison[9]. A comparision with the only available experimental results by Delage and Carette[8] shows a good agreement for this state, as well as for $5s\ [3/2]_1$.

For the $5p\ [1/2]_0$ state the only available experimental result is by Delage and Carette[8]. It is not simple to discuss the agreement in shape due to a limited amount of data points obtained by these authors, especially in domain of the minimum. It is clear that our result of inelastic-to-reference inelastic intensity ratio for the 5p state is larger than result of Delage and Carette[8].

Thus, on the basis of normalized elastic DCS values as well as the separately measured elastic-to-reference inelastic ($5s\ [3/2]_1$ state) intensity ratio, the absolute inelastic DCS values for the krypton atom were obtained for: $5s\ [3/2]_1$, $5s'\ [1/2]_1$ and $5p\ [1/2]_0$ states. These DCS values were obtained in the wide angular range from 10° to 150° for the first time, and presented in this paper.

Acknowledgements

We would like to thank Professor Milan Kurepa for many fruitful disucssions and contribution to the building of the spectrometer, Dr Slobodan Cvejanović for helping with the electronics and Predrag Jovanović for helping with the construc-

tion of the apparatus. This work has been supported by the Republic Council of Scientific Research of Socialist Republic of Serbia, Yugoslavia, and partly by the National Bureau of Standards (Grant No. J P 598) USA.

References

1) N. Andersen, J. W. Gallagher and U. V. Hertel, in *Invited Papers of the Fourteenth International Conference on the Physics of Electronic and Atomic Collisions,* edited by D. C. Lorents, W. E. Meyerhof and J. R. Peterson, Palo Alto, North Holland (1986), p. 57; and private communication (1985);
2) I. McGregor, D. Hils, R. Hippler, N. A. Malik, J. F. Williams, A. A. Zaidi and H. Kleinpoppen, J. Phys. B **15** (1982) 1411;
3) H. Nishimura, A. Danjo, T. Koike, K. Kani, H. Sugahara and A. Takahashi, in *Electron--Molecule Collisions and Photoionization Processes;* Proc. of the First United States-Japan Seminar, edited by V. McKoy, H. Suzuki, K. Takayanagi and S. Trajmar (Chemie, Dearfield Beach, Florida, 1982);
4) G. D. Meneses, F. J. da Paixão and N. T. Padial, Phys. Rev. A **32** (1985) 156;
5) B. R. Lewis, E. Weigold and P. J. O. Teubner, J. Phys. B **8** (1975) 212;
6) A. Delage and J. D. Carette, Can. J. Phys. **53** (1975) 2079;
7) P. S. Ganas and A. E. S. Green, Phys. Rev. A **4** (1971) 182;
8) A. Delage and J. D. Carette, Can. J. Phys. **55** (1977) 1835;
9) K. Bartschat and D. H. Madison, J. Phys. B **20** (1987) 5839;
10) D. Filipović, V. Pejčev, B. Marinković and L. Vušković, in *Book of Abstracts of the Second European Conference on Atomic and Molecular Physics,* edited by A. E. de Vries and M. J. van der Wiel (ECAMP, Amsterdam, 1985), p. 67;
11) D. Filipović, B. Marinković, V. Pejčev and L. Vušković, Phys. Rev. A **37** (1988) 356;
12) B. Marinković, Cz. Szmytkowski, V. Pejčev, D. Filipović and L. Vušković, J. Phys. B **19** (1986) 2365;
13) L. Vušković, D. Filipović and V. Pejčev, in *Book of Abstracts of the Eight International Conference on Atomic Physics,* edited by I. Lidgren, A. Rosen and S. Svanberg (Göteborg, 1982), p. 105;
14) B. Marinković, V. Pejčev, D. Filipović and L. Vušković, in *Book of Abstracts of the Fifteenth International Conference on the Physics of Electronic and Atomic Collisions,* edited by J. Geddes, H. B. Gilbody, A. E. Kingston, C. J. Latimer and M. J. R. Walters (Brighton, 1987), p. 186;
15) B. Marinković, V. Pejčev and L. Vušković, in *Book of Abstracts of the Nineteenth Europhysics Conference,* edited by S. Mathfessel and G. Thomas (EGAS, Dublin, 1987), C3-17;
16) A. Chutjian, J. Chem. Phys. **61** (1974) 4279;
17) C. E. Kuyatt, *Electron Optics Lectures,* unpublished notes lecture, NBS, Washington D. C. (1967);
18) D. Filipović, S. Kazakov, B. Marinković, Cz. Szmytkowski, V. Pejčev and L. Vušković, in *Book of Contributed Papers of the Thirteenth International Symposium on the Physics of Ionized Gases,* edited by M. V. Kurepa (Šibenik, 1986), p. 3;
19) S. K. Srivastava, H. Tanaka, A. Chutjian and S. Trajmar, Phys. Rev. A **23** (1981) 2156.

POBUĐIVANJE KRIPTONA U SUDARU SA ELEKTRONIMA ENERGIJE 60 eV

DUŠAN FILIPOVIĆ, VLADIMIR PEJČEV, BRATISLAV MARINKOVIĆ i LEPOSAVA VUŠKOVIĆ

Institut za Fiziku, P. P. 57, 11001 Beograd

UDK 539.186

Originalan naučni rad

Normalizovani, apsolutni diferencijalni preseci (DCS-i) za neelastično rasejanje elektrona energije 60 eV na atomu kriptona izmereni su za stanja: 5s $[3/2]_1$, 5s' $[1/2]_1$, te 5p $[1/2]_0$. Energijsko razlaganje spektrometra bilo je oko 50 meV, a uglovi rasejanja od 10° do 150°. DCS-i izmereni su u širokom ugaonom intervalu po prvi put u ovome radu. Opisane su osobine korišćenog elektronskog spektrometra.